Research Article | Vol. 10, No. 5 / 1 May 2020 / Optical Materials Express 1264
Optical Materials EXPRESS

# Label-free biomechanical nanosensor based on LSPR for biological applications

M. Salbini,[1,2,*] T. Stomeo,[1] C. Ciracì,[1] R. Fiammengo,[1] V. Mangini,[1] A. Toma,[3] F. Pisano,[1] F. Pisanello,[1] T. Verri,[2] D. R. Smith,[4] and M. De Vittorio[1,5]

[1]Center for Biomolecular Nanotechnologies, Istituto Italiano di Tecnologia, Arnesano (Lecce), Italy
[2]Dipartimento di Scienze e Tecnologie Biologiche e Ambientali, Università del Salento, Lecce, Italy
[3]Istituto Italiano di Tecnologia, Genova, Italy
[4]Center for Metamaterials and Integrated Plasmonics, Duke University, Durham, NC 27708, USA
[5]Dipartimento di Ingegneria dell'Innovazione, Università Del Salento, Lecce, Italy
*maria.salbini@iit.it

**Abstract:** A label-free localized surface plasmon resonance (LSPR)-based biosensor exploiting gold nanorods (GNRs) is proposed and demonstrated. For this aim, 35 ± 5 nm long and 20 ± 4 thick GNRs spaced by a few nanometers thick polyelectrolytes (PE) from a gold thin film was analyzed and synthesized. The morphology of the GNRs, the plasmon properties of GNRs, swelling of PE layers and the wettability of the surfaces were characterized by transmission and scanning electron microscopy, spectroscopic reflectivity and contact angle measurements, respectively. Indeed, when immersed in a phosphate buffer saline solution, the GNRs-PE-gold system shows an optical shift of the LSPR wavelength. This shift was found to correspond to a vertical swelling of about 2 nm, demonstrating the extreme sensitivity of the biosensor. Finally, we show that LSPR measurements can be used to detect dynamic resonance changes in response to both thickness and buffer solution, while the hydrophobic behavior of the surface can be exploited for reducing the number of liquid analytes in clinical biosensing application.



## 1. Introduction

*Localized surface plasmons* (LSP) are collective oscillations of free electrons in a noble metal arising when light impinges on metallic nanoparticles [1]. The scattering and absorption properties of the excited plasmons depend on the type of metal, size and shape of the nanostructure, refractive index of the surrounding environment and wavelength of light [1–3]. Various metal nanostructures with controlled shape and size have been fabricated and applied within the plasmonics framework [4,5]. Among them, gold nanorods (GNRs) have emerged as convenient material that supports LSPR at longer wavelength. However, these nanoparticles are unstable due to their high surface energy, and therefore require suitable surface modifications for their stabilization, which will prevent aggregation [6,7]. The plasmonic response tuning range can be further increased by plasmonic hybridization between self-similar particles [8,9] or between nanoparticles and a metallic surface [10–14]. Polyelectrolytes (PEs) with controlled thickness are often used to produce controllable dielectric layers between nanoparticles and the metallic film [15]. GNRs-PE-films and LSPR have been already applied to monitor the pH of biological fluids by an optical setup. The swelling behavior of PE films can be applied to nanomaterial construction, enzyme immobilization [16] and to detect differences between proteins exploiting different sizes and charges [17].

In this work, we report on the design, fabrication, characterization and calibration of a GNRs-PE-film exploiting LSPR coupling. We employ GNRs spaced by a few nanometers thick PE layer from a metallic film and exploit the strong distance-dependent GNRs-PE-film coupling to measure a shift in the resonance of the system as a function of the dielectric spacer swelling.

#385713 https://doi.org/10.1364/OME.385713
Journal © 2020 Received 10 Dec 2019; revised 31 Jan 2020; accepted 1 Feb 2020; published 17 Apr 2020

Optical Materials EXPRESS

Isolated GNRs have two plasmon resonances: a transverse one, corresponding to a wavelength of ~ 526 nm and a longitudinal one at a longer wavelength (in this study 692 nm), whose position is determined by the aspect ratio of the nanorods. Characterization results, including scanning and transmission electron microscopy, darkfield microscopy, optical reflection spectra and contact angle measurements, highlight the ability of the device of real-time and label-free sensing. The proposed system fabrication and its advantages for detecting dynamic resonances changes in response to both thickness and different solution variations are discussed.

## 2. Experimental section

### 2.1. Materials

Cetyltrimethylammonium bromide (CTAB, ≥ 99%), gold (III) chloride trihydrate (HAuCl4 • 3H2O, ≥ 99%), silver nitrate (AgNO3, ≥ 99%), sodium borohydride (NaBH4, ≥ 99%), poly (allylamine hydrochloride) (PAH, Mw ~17,500) and polystyrene sulfonate (PSS, 18 wt. % in H2O, Mw ~75,000) were purchased from Sigma Aldrich. Ascorbic acid (ACS grade) was purchased from ACROS. Hydrochloric acid (HCl, certified 1 M) was purchased from J.T. BAKER.

### 2.2. Synthesis of gold nanorods

A seeds solution was prepared according to the methods reported in [18]. Briefly, 62.5 µL of 0.01 M of gold (III) chloride trihydrate (HAuCl4 • 3H2O) in water was added to 2.5 mL of 0.1 M of hexadecyltrimethylammonium bromide (CTAB) in water at 25 - 30° C. 150 µL of ice-cold, freshly prepared 0.01 M of sodium borohydride (NaBH4) was added at once to the stirred gold/CTAB solution resulting immediately in a yellowish brown color. After 2 min stirring, the solution was incubated at 37° C for 1 h. A growth solution was prepared adding 0.388 mL of 0.01 M of silver nitrate (AgNO3), 2.5 mL of 0.01 M of gold (III) chloride trihydrate (HAuCl4 • 3H2O), 2.0 mL of 1.0 M HCl, to 50 mL of 0.1 M CTAB solution at 30 °C. The growth mixture was gently stirred for 15 min before the addition of 0.4 mL of freshly prepared 0.1 M ascorbic acid solution in water. After approx. 30 sec vigorous stirring the solution turned colorless and was injected with 75 µL of the previously prepared seed solution. The GNRs were grown at 25° C overnight. The GNRs were purified by centrifugation at 20000×g for 20 min. at 27° C. Most of the supernatant solution was removed leaving approx. 1 mL and the residue was added to 10 mL water. The centrifugation step was repeated twice-affording approx. 3 mL of final GNRs solution (1270 µg Au/mL).

After synthesis, the CTAB protected GNRs were coated with ((1-mercaptoundec-11-yl) PEG600)-acetic acid in a two-step procedure to remove the CTAB efficiently. Briefly, in the first step, 3.0 mL of GNRs were mixed with 0.4 mL 200 mM acetate buffer pH 4.5, 0.6 mL of water, 2.0 mL of ethanol, and 2.1 mL of 5 mM PEG thiol. The reaction mixture was stirred at room temperature for 4 days and then the nanoparticles were purified by centrifugation and resuspension in water/ethanol 80:20 (2×, 8800×g for 10 min. at 20° C) and in water (2×, 8800×g for 10 min. at 20° C). This procedure afforded 1.0 mL of intermediate GNRs solution, which was used directly in a second coating step. In this case, the GNRs solution was added to a mixture of 0.8 mL of 5 mM PEG thiol, 0.333 mL 300 mM carbonate buffer, and 1.86 mL of water. After 4 days stirring at room temperature, the GNRs were purified by centrifugation and resuspension in 4 mL water (2×, 5000×g for 20 min. at 20° C), ultrafiltration (Amicon Ultra-4 Centrifugal Filter Units, regenerated cellulose – 100 kDa from Millipore) washing with 10 mM NaHCO3/ethanol 80:20 (3 × 4 mL), 10 mM NaHCO3 (1 × 4 mL), and with water (1 × 4 mL). The GNRs were taken up in 0.344 mL of water and further purified via gel filtration (Illustra NAP-10 columns from GE Healthcare) obtaining 1.5 mL of purified, PEG-coated, GNRs in water (approx. 600 µg Au/mL).

Optical Materials EXPRESS

#### 2.2.1. GNRs characterization

UV/Vis measurements were carried out using a TECAN Infinite M200 Pro plate reader or a Cary 5000 spectrophotometer. The UV-Vis spectrum of a representative GNR sample is shown in Fig. 1(A). GNRs were imaged via TEM (JEOL JEM-1011 transmission electron microscope operating at an accelerating voltage of 100 kV, Fig. 1(B)). The geometrical characteristics of the GNRs were determined by evaluating the TEM images with the software Image J. [18] The GNRs used in this work were 35 ± 5 nm long and 20 ± 4 thick. The concentration of gold was determined via inductively coupled plasma-optical emission spectroscopy (Agilent 720 ICP-OES). The measured gold concentrations (µg Au/mL) were converted into particle concentration (nanomolar, nM) assuming the shape of a GNR to be a cylinder with spherical caps.

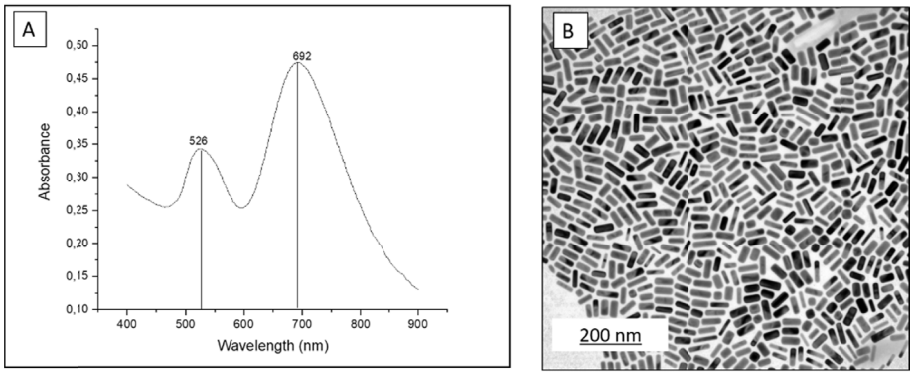


**Fig. 1.** (A) UV-Vis-NIR spectrum of GNRs. (B) TEM image of GNRs as fabricated.

### *2.3. Polyelectrolyte (PE)-based spacer layer preparation and gold nanorods deposition*

Thin gold films (50 nm) were deposited onto a silicon wafer by an electron beam evaporation, using a 5 nm thick titanium film as an adhesion layer. Samples were cut to size before the deposition of the polyelectrolyte (PE)-based spacer layer and the GNRs.

Gold film on the samples was cleaned rinsing with acetone and isopropyl alcohol and finally dried with nitrogen gas. The PE-based spacer layer was obtained by Layer-by-Layer (LBL) deposition [19,20] alternating positively charged poly (allylamine hydrochloride) (PAH, 15,000 g/mL) and negatively charged polystyrene sulfonate (PSS, 75, 00 g/mL, 18% wt in H2O). The gold-coated substrates were immersed in an aqueous solution containing 0.003 mol of monomer/L PE and 1 M sodium chloride (NaCl) for 5 minutes, rinsed thoroughly with a gentle stream of ultrapure water and immersed in fresh 1 M NaCl for 1 minute. The substrates were again washed with ultrapure water before each subsequent deposition step of an oppositely charged PE. Finally, the samples were gently dried with a stream of high purity nitrogen gas. We choose the 5 min deposition time for the PE layer films based on Moreau et al. [10] protocol, that demonstrates that the thickness of the polyelectrolyte layer is around 1 nm before deposition of the nanoparticles. Aqueous solutions of PSS and PAH in 1 M NaCl were at pH 5.7 and 6.0, respectively. LBL deposition always started and finished with the cationic PAH layer to facilitate the attachment to the gold film [20,21] and the immobilization of the ((1-mercaptoundec-11-yl) PEG600)-acetic acid- coated GNRs via electrostatic interactions.

Deposition of the GNRs onto the PE spacer layer was done by drop casting, i.e. delivering the undiluted GNR solution onto the samples surface, followed by an incubation time of 1 hour. Afterward, the samples were rinsed with ultrapure water and dried with a stream of high-purity

Optical Materials EXPRESS

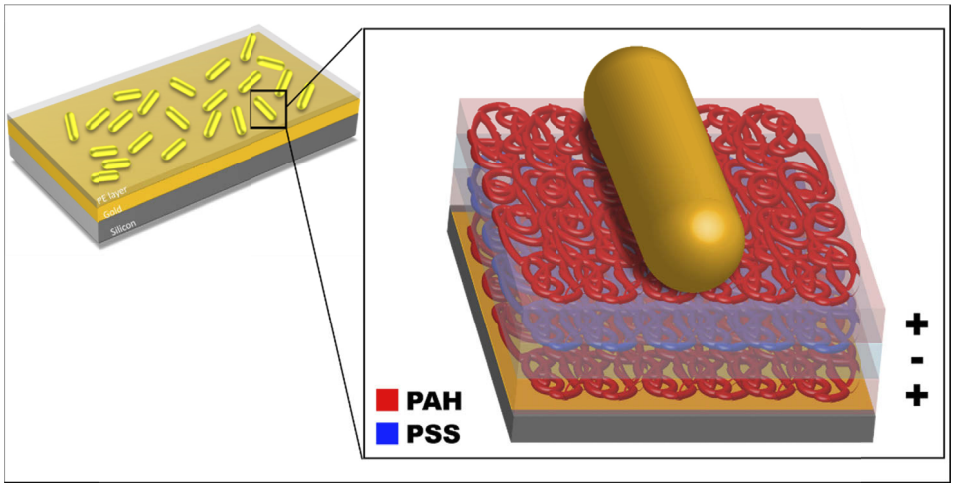


**Fig. 2.** Schematic representation of the GNRs-PE-film sample (not in scale).

nitrogen. A schematic representation of the final GNRs-over-metal film system is depicted in Fig. 2.

#### 2.3.1. Gold nanorods-film plasmonic characterization

After GNR deposition, morphological characterization of the final sample was carried out by scanning electron microscopy (SEM) on a Dual Beam FIB/SEM Heli-osNanoLab600i instrument (Fig. 3(A)). The electron micrographs show that GNRs are randomly oriented on the surface of the sample. Nevertheless, their random orientation is not expected to cause any problem because it is well known that the pattern does not affect the resonance properties of the system [10].

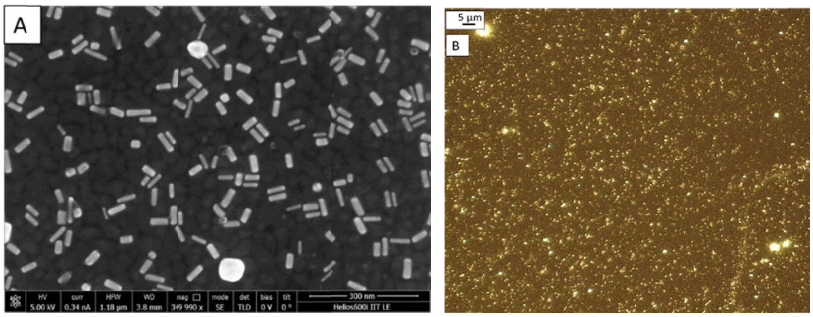


**Fig. 3.** (A) SEM image of GNRs adsorbed on the thin gold film sample;(B) Dark-field scattering images of gold nanorods adsorbed on a thin gold film; PE layer thickness: thickness 3 nm.

The plasmonic properties of the GNRs-PE-film decorated samples were investigated via optical reflectivity. Scattering measurements were performed on all samples characterized by different thickness of the PE-spacer layer via dark-field microscopy. Figure 3(B) show the typical dark-field scattering images for GNRs adsorbed on 3 nm of PE-spacer layers on top of a thin gold film [22].

Optical Materials EXPRESS

### 2.3.2. Sensor surface characterization

The surface wettability for samples decorated with GNRs or without GNRs was investigated determining the contact angle with the sessile drop method [23] by means of an OCA 15Pro Contact Angle Tool (Data Physics) instrument. Contact angles were measured using either water or phosphate buffered saline (PBS, pH 7, 4) solution and the reported values are averages of three independent measurements. The drop images and the results of wettability measurements are reported in Fig. 4, where similar behavior has been observed using water (Fig. 4(A)) or PBS (Fig. 4(B)). The presence of GNRs decreases the contact angle to lower values, with a difference of ~20° between the surfaces not presenting and those presenting gold nanorods. As expected, the degree of wetting and its properties are closely linked to surface morphology and roughness. This difference confirms that by adding GNRs the surface keeps its hydrophilic behavior, necessary for both pH detection and monitoring in any aqueous solution.

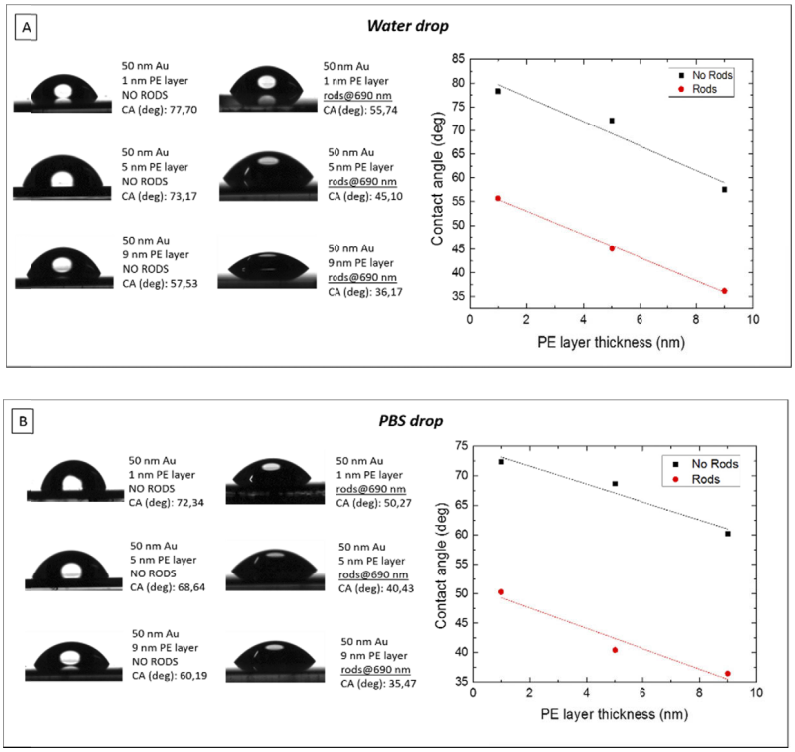


**Fig. 4.** Wettability measurements in sessile-drop mode: (A) with water drop, (B) with PBS drop.

## 2.4. *Optical setup for swelling studies*

The PE-based spacer layer may undergo swelling depending on the characteristics of the solution in which it is equilibrated. A custom-made optical setup was used to investigate the swelling behavior of the PE-layer. Broadband, incoherent light (Ocean Optics HL 2000) passing through a 100 µm pinhole was collimated with a lens (focal 250 mm), reflected by a beam splitter (50/50) and focused on the sample with a low numerical aperture (NA), infinity-corrected objective (5x, 0.13 NA). The reflected light passing, through the beam splitter, was injected into a multimode optical fiber with an objective lens (20x, NA 0.5) and sent to a spectrometer (Horiba Scientific iHR320) equipped with an EMCCD camera (Horiba Scientific Synapse, 1600 × 200 pixels. The

Optical Materials EXPRESS

plasmonic properties of the multilayer films were examined at different time points during PBS immersion. Then, the films were dried to examine whether swelling influences the dry-state thickness and to determine a "molecular memory" caused by previous treatment [24].

## 3. Results and discussion

Here we present, plasmonic structures composed of colloidally synthesized GNRs spaced by a few nanometers thick PE from a gold thin film.

There are several appealing nanoscale properties of this plasmonic architecture. For example, the plasmon resonance between the metal nanorods and the film can be controlled precisely by varying the thickness of the PE spacer layer and the size of the rods. The resonance can be tuned virtually anywhere from 800 to 1500 nm. We created a GNR-PE-film coupling sample with 50 nm of thin gold film, a PE spacer layer of different thicknesses (1 to 9 nm) and gold nanorods on top. The spacer layer between the nanorods and the gold film is completely transparent at visible and near-infrared wavelengths. Consequently, the observed absorption is due exclusively to ohmic losses in the metal and scattering. In each case, the sample spectrum can be normalized with respect to a blank spectrum of a gold film containing the respective PE layer and no immobilized GNRs.

As typical with such nano-plasmonic systems, resonances are extremely sensitive to the thickness and dielectric properties of the spacer layer, thus providing an effective way to optically measure the gap dimension [11]. Based on our simulations, we expect a measurable reflectance signal even for low GNRs surface coverage. The NIR optical response is shown in Fig. 5(A), where changes in the refractive index (RI) of the nanoparticles surrounding medium (due to the gap size increase) induced a clear blue shift in the LSPR position (Fig. 5(A) and Fig. 5(B)). These measurements have been performed by UV-3600 spectrometer, Shimadzu.

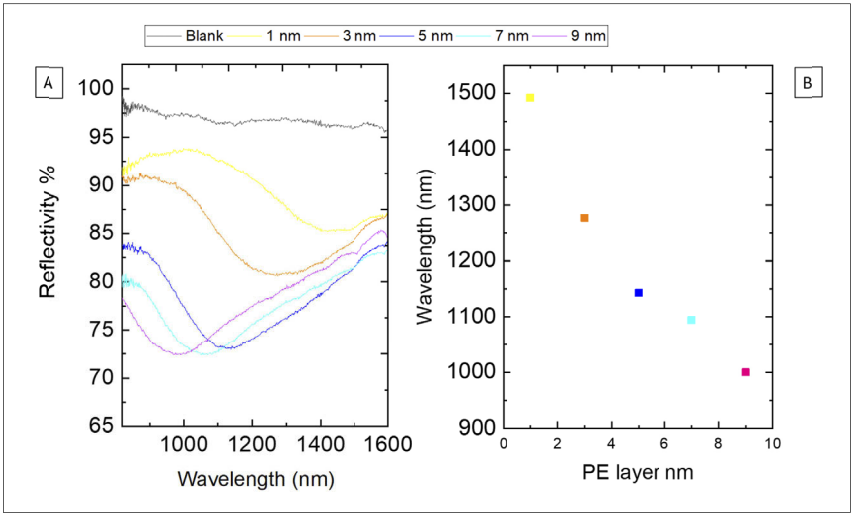


**Fig. 5.** Experimental results of the tunability of the reflectance (A) and the position of the resonance as a function of the spacer thickness (B).

Typically, a biosensor based on nanostructures and metallic films separated by PE layers face significant challenges to be used in an aqueous solution. Thank our setup, we used the GNRs-PE-film system to deduce sub-nanometer changes in the PE layer thickness by measuring the LSPR shift in response to different aqueous solutions. It is well known that PE multilayers containing at least one weak PE, such as PAH, will swell and deswell in response to PBS solution

Optical Materials EXPRESS

[25] because of protonation and deprotonation as a function of the buffer. A custom-made setup was initially used for measuring the GNRs-PE-film sample in air (dry state).

Figure 6 shows representative GNRs-PE-film SPR data at different time points during buffer immersion and after dry state. We have tested our samples by using three different buffer solutions: Phosphate buffer saline (PBS, 10mM phosphate, 137 Mm NaCl, pH 7), carbonate buffer (CB, 10mM sodium carbonate, pH 7.5) and carbonate buffer saline (CBS, 10 mM sodium carbonate, 137mM NaCl, pH 7.5). We decided to use CB, both with and without NaCl 137 mM, for investigating in the same condition if the swelling is due to Ionic Strength.

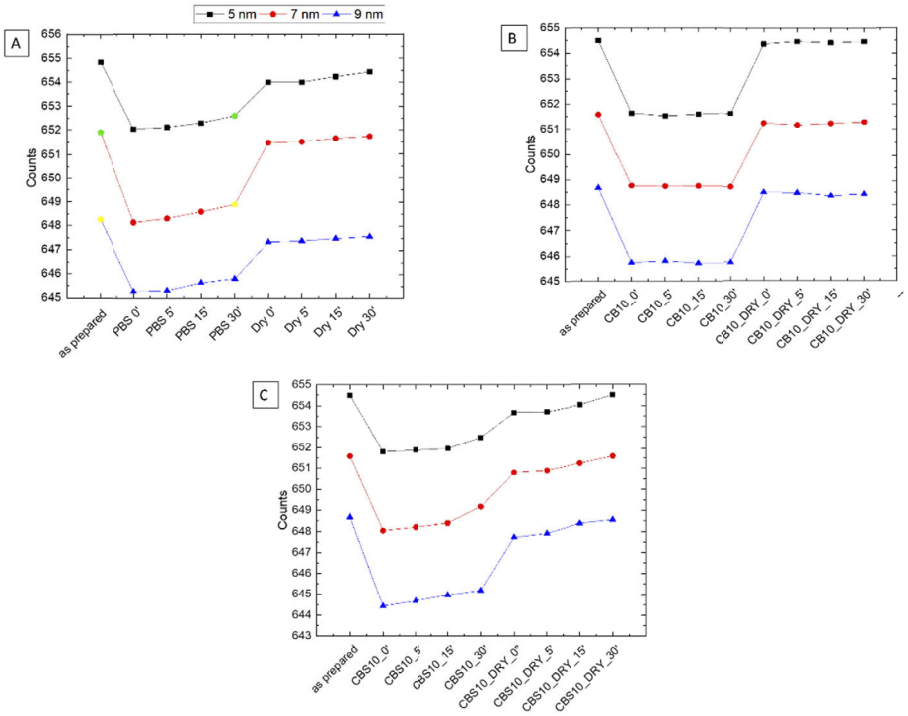


**Fig. 6.** The GNRs-PE-film SPR peak centroids are plotted over time, indicating semi-reversible induced swelling in during immersion in three different buffer: (A) PBS, (B) Carbonate and (C) carbonate with NaCl. All the study was made with 3 different PE layer spacer layer thickness, 5- and 9 nm.

We started to control the effect of PBS only without swelling, at 'time 0', just to see the effect of medium changing. Then we noted that the GNR-film samples immersed in PBS solution revealed a blue-shit of the resonance, due to the PE layer swelling. After drying the sample, a red shift behavior occurs, caused by the deswelling of the PE layer. The SPR peak wavelength as a function of time shows that there is a semi reversible trend in the peak counts. At the same time, the system does not show any significant molecular memory when dried after the PBS treatment. This particular performance was verified in 5, 7 and 9 nm PE layer samples. Based on these observations, the position of the plasmon resonance observed in our experiment is most likely due to the increasing and decreasing of the thickness of the PE layer. In Fig. 6(A), it is shown that immersion in PBS for 30 min of a 5 nm thick PE layer leads to an SPR resonance corresponding to that of a 7 nm thick unswollen sample. The thickness increase as a consequence of the swelling process is therefore about ~ 2 nm. The same behavior is observed for 7nm and 9 nm PE layers.

The experimental results show also that by using only CB no swelling occurs (Fig. 6(B)). Instead, when CBS is used, the same swelling behavior of the PBS buffer is achieved (Fig. 6(C)).

Optical Materials EXPRESS

These results show that the PE layer thickness is dependent on the ionic strength, [26,27].

## 4. Conclusions

We have illustrated the design and fabrication of an optical biosensor composed of GNRs spaced by a few nanometers thick PE layer from a gold thin film. Our LSPR based biosensor is label-free and shows high sensitivity to the local refractive index change, pointing out the potential for multiplexed sensing and the capability of working as a biochemical sensor

The experimental on our architecture highlights that the observed resonances can be related to the PE layer thickness and dielectric properties confirming that changes in the refractive index of the GNRs surrounding medium induce a shift in the LSPR peak position. In addition, the sensor can measure the effect of the buffer solution through swelling monitoring. Indeed, a 2 nm swelling, results in an LSPR wavelength shift of 2 nm due to PBS, at pH 7.4. The system goes back to its previous state when the sample is dried, because of the PE layers deswelling, without any significant "molecular memory". In line with this, the present results envision significant perspectives for label-free LSPR biosensing to evaluate cell performances, such as force generation or proteins and enzymes characterization.

## Acknowledgments

F. Pisano and F. Pisanello acknowledge funding from the European Research Council under the European Union's Horizon 2020 research and innovation program (#677683); M.D.V. acknowledges funding from the European Research Council under the European Union's Horizon 2020 research and innovation program (#692943). F. Pisanello acknowledges that project leading to this application has received funding from the European Union's Horizon 2020 research and innovation programme under grant agreement No 828972. M.D.V. is funded by the US National Institutes of Health (U01NS094190). M.D.V. is funded by the US National Institutes of Health (1UF1NS108177-01).

## Disclosures

The authors declare no conflicts of interest.

## References

1. K. M. Mayer and J. H. Hafner, "Localized Surface Plasmon Resonance Sensors," Chem. Rev. **111**(6), 3828–3857 (2011).
2. K. A. Willets and R. P. Van Duyne, "Localized surface plasmon resonance spectroscopy and sensing," Annu. Rev. Phys. Chem. **58**(1), 267–297 (2007).
3. G. J. Nusz, S. M. Marinakos, A. C. Curry, A. Dahlin, F. Höök, A. Wax, and A. Chilkoti, "Label-free plasmonic detection of biomolecular binding by a single gold nanorod," Anal. Chem. **80**(4), 984–989 (2008).
4. X. Xia, J. Zeng, Q. Zhang, C. H. Moran, and Y. Xia, "Recent Developments in Shape-Controlled Synthesis of Silver Nanocrystals," J. Phys. Chem. C **116**(41), 21647–21656 (2012).
5. G. K. Joshi, P. J. McClory, B. B. Muhoberac, A. Kumbhar, K. A. Smith, and R. Sardar, "Designing Efficient Localized Surface Plasmon Resonance-Based Sensing Platforms: Optimization of Sensor Response by Controlling the Edge Length of Gold Nanoprisms," J. Phys. Chem. C **116**(39), 20990–21000 (2012).
6. R. Pang, S. Zhou, X. Hu, Z. Xie, X. Liu, H. Duadi, and D. Fixler, "New diffusion reflection imaging system using gold nanorods coated with poly-(3,4-ethylenedioxythiophene)," Opt. Mater. Express **6**(4), 1238–1246 (2016).
7. R. Ankri and D. Fixler, "Gold nanorods based diffusion reflection measurements: current status and perspectives for clinical applications," Nanophotonics **6**(5), 1031–1042 (2017).
8. P. Nordlander, C. Oubre, E. Prodan, K. Li, and M. I. Stockman, "Plasmon Hybridization in Nanoparticle Dimers," Nano Lett. **4**(5), 899–903 (2004).
9. E.-M. Roller, C. Argyropoulos, A. Högele, T. Liedl, and M. Pilo-Pais, "Plasmon–Exciton Coupling Using DNA Templates," Nano Lett. **16**(9), 5962–5966 (2016).
10. A. Moreau, C. Ciracì, J. J. Mock, R. T. Hill, Q. Wang, B. J. Wiley, A. Chilkoti, and D. R. Smith, "Controlled-reflectance surfaces with film-coupled colloidal nanoantennas," Nature **492**(7427), 86–89 (2012).
11. G. M. Akselrod, J. Huang, T. B. Hoang, P. T. Bowen, L. Su, D. R. Smith, and M. H. Mikkelsen, "Large-Area Metasurface Perfect Absorbers from Visible to Near-Infrared," Adv. Mater. **27**(48), 8028–8034 (2015).

Optical Materials EXPRESS


12. J. Mertens, A. L. Eiden, D. O. Sigle, F. Huang, A. Lombardo, Z. Sun, R. S. Sundaram, A. Colli, C. Tserkezis, J. Aizpurua, S. Milana, A. C. Ferrari, and J. J. Baumberg, "Controlling Subnanometer Gaps in Plasmonic Dimers Using Graphene," Nano Lett. **13**(11), 5033–5038 (2013).
13. J. J. Mock, R. T. Hill, A. Degiron, S. Zauscher, A. Chilkoti, and D. R. Smith, "Distance-Dependent Plasmon Resonant Coupling between a Gold Nanoparticle and Gold Film," Nano Lett. **8**(8), 2245–2252 (2008).
14. C. Ciracì, X. Chen, J. J. Mock, F. McGuire, X. Liu, S.-H. Oh, and D. R. Smith, "Film-coupled nanoparticles by atomic layer deposition: Comparison with organic spacing layers," Appl. Phys. Lett. **104**(2), 023109 (2014).
15. R. T. Hill, K. M. Kozek, A. Hucknall, D. R. Smith, and A. Chilkoti, "Nanoparticle–Film Plasmon Ruler Interrogated with Transmission Visible Spectroscopy," ACS Photonics **1**(10), 974–984 (2014).
16. C. L. Cooper, P. L. Dubin, A. B. Kayitmazer, and S. Turksen, "Polyelectrolyte–protein complexes," Curr. Opin. Colloid Interface Sci. **10**(1-2), 52–78 (2005).
17. Y. Fan, S. Tang, E. L. Thomas, and B. D. Olsen, "Responsive Block Copolymer Photonics Triggered by Protein–Polyelectrolyte Coacervation," ACS Nano **8**(11), 11467–11473 (2014).
18. H.-H. Chang and C. J. Murphy, "Mini Gold Nanorods with Tunable Plasmonic Peaks beyond 1000 nm," Chem. Mater. **30**(4), 1427–1435 (2018).
19. G. Decher, "Fuzzy Nanoassemblies: Toward Layered Polymeric Multicomposites," Science **277**(5330), 1232–1237 (1997).
20. Z. Tang, Y. Wang, P. Podsiadlo, and N. A. Kotov, "Biomedical Applications of Layer-by-Layer Assembly: From Biomimetics to Tissue Engineering," Adv. Mater. **19**(7), 906 (2007).
21. A. Noy, C. D. Frisbie, L. F. Rozsnyai, M. S. Wrighton, and C. M. Lieber, "Chemical Force Microscopy: Exploiting Chemically-Modified Tips To Quantify Adhesion, Friction, and Functional Group Distributions in Molecular Assemblies," J. Am. Chem. Soc. **117**(30), 7943–7951 (1995).
22. K.-S. Lee and M. A. El-Sayed, "Dependence of the Enhanced Optical Scattering Efficiency Relative to That of Absorption for Gold Metal Nanorods on Aspect Ratio, Size, End-Cap Shape, and Medium Refractive Index," J. Phys. Chem. B **109**(43), 20331–20338 (2005).
23. J. E, Y. Jin, Y. Deng, W. Zuo, X. Zhao, D. Han, Q. Peng, and Z. Zhang, "Wetting Models and Working Mechanisms of Typical Surfaces Existing in Nature and Their Application on Superhydrophobic Surfaces: A Review," Adv. Mater. Interfaces **5**(1), 1701052 (2018).
24. K. Itano, J. Choi, and M. F. Rubner, "Mechanism of the pH-Induced Discontinuous Swelling/Deswelling Transitions of Poly(allylamine hydrochloride)-Containing Polyelectrolyte Multilayer Films," Macromolecules **38**(8), 3450–3460 (2005).
25. G. Jiang, A. Baba, H. Ikarashi, R. Xu, J. Locklin, K. R. Kashif, K. Shinbo, K. Kato, F. Kaneko, and R. Advincula, "Signal Enhancement and Tuning of Surface Plasmon Resonance in Au Nanoparticle/Polyelectrolyte Ultrathin Films," J. Phys. Chem. C **111**(50), 18687–18694 (2007).
26. S. Dodoo, B. N. Balzer, T. Hugel, A. Laschewsky, and R. v. Klitzing, "Effect of Ionic Strength and Layer Number on Swelling of Polyelectrolyte Multilayers in Water Vapour," Soft Mater. **11**(2), 157–164 (2013).
27. M. Kolasińska, R. Krastev, T. Gutberlet, and P. Warszyński, "Swelling and Water Uptake of PAH/PSS Polyelectrolyte Multilayers," in: G. K. Auernhammer, H.-J. Butt, and D. Vollmer, eds. *Surface and Interfacial Forces – From Fundamentals to Applications* (Springer Berlin Heidelberg, 2008), pp. 30–38.